Available online at www.sciencedirect.com
ScienceDirect
Journal of Molecular Graphics and Modelling 26 (2008) 893–899
Journal of Molecular Graphics and Modelling
www.elsevier.com/locate/JMGM

Structural, electronic, and magnetic properties of two isomers of $C_{40}O_{10}$ with cage-like structure

Feng-Ling Liu *, Chen-Hui Wang

College of Chemistry, Chemical Engineering and Materials Science, Engineering Research Center of Pesticide and Medicine Intermediate Clean Production, Ministry of Education, Shandong Normal University, Jinan 250014, People's Republic of China

Received 29 April 2007; received in revised form 7 June 2007; accepted 8 June 2007
Available online 14 June 2007

Abstract

Bonding, vibrational and magnetic properties of two isomers of cage-like molecule $C_{40}O_{10}$ are studied by using hybrid DFT calculations at the B3LYP/6-31G* level of theory. Infrared- and Raman-active vibrational frequencies of two isomers of $C_{40}O_{10}$ are assigned. Three ^{13}C and one ^{17}O nuclear magnetic resonance (NMR) spectral signals of each isomer are characterized. Heat of formation of each isomer is estimated. Compared the stability of the two isomers of $C_{40}O_{10}$ with that of C_{60}, only from the thermodynamic points of view, they are more stable than C_{60}. Thus, we believe that they have sufficient stability to allow their experimental preparation. We proposed their synthesized route in this paper.

Keywords: Cage-like molecule $C_{40}O_{10}$; B3LYP/6-31G*; Vibrational frequency; NMR; Heat of formation

1. Introduction

In 1971, Barth and Lowton reported the synthesis of corannulene $C_{20}H_{10}$ (Fig. 1) [1]. If all hydrogen atoms in corannulene $C_{20}H_{10}$ are substituted by OH group or chlorine atoms, $C_{20}(OH)_{10}$ and $C_{20}Cl_{10}$ can be obtained. If the following condensation reaction take place:

$$C_{20}(OH)_{10} + C_{20}Cl_{10} = C_{40}O_{10} + 10HCl$$

the molecule $C_{40}O_{10}$ with cage-like structure generated. To the author's knowledge, nothing at all is known about the molecule $C_{40}O_{10}$ with cage-like structure. The molecule $C_{40}O_{10}$ has two isomers, and their structures are shown in Fig. 2. We study the molecule $C_{40}O_{10}$ firstly to extend range of cage-like molecule, second to look for the cage-like molecules that have some hydrophilic property.

From Fig. 2, it can be seen that the shape of the molecule $C_{40}O_{10}$ likes an oblate sphere, and all oxygen atoms are at the equator of the cage. The isomer 1 contains 2 pentagons, 15 hexagons and 5 octagons, of which 5 hexagons and all octagons contain oxygen atoms. The isomer 2 contains 2 pentagons, 10 hexagons and 10 heptagons, of which all heptagons contain oxygen atoms. This current work is a theoretical attempt to study the two isomers of the molecule $C_{40}O_{10}$ by using the hybrid DFT method at the B3LYP/6-31G* level of theory [2]. For future experimental identification of the two isomers, their vibrational frequencies and the magnetic shielding tensors are calculated. For the sake of understanding the thermodynamic stability, their heats of formation ΔH_f° were estimated in this paper.

2. Computational details

The full geometry optimization for the two isomers of the molecule $C_{40}O_{10}$ was performed by using the energy gradient method at the B3LYP/6-31G* level of theory. Since the polarization functions are essential for the realistic expression of geometries of the molecules involving second row elements [3], the basis set of 6-31G* as used in this study. The asterisks (*) indicate that six d-type polarization functions for carbon and oxygen atoms were included in the 6-31G* basis sets. We have carried out all calculations using Gaussian 98 program system [4]. After the optimization of the geometry, the symmetries of

* Corresponding author at: Shandong Normal University, Jinan 250014, People's Republic of China. Tel.: +86 531 86180743; fax: +86 531 82615258.
E-mail address: sdliufl@sina.com (F.-L. Liu).

1093-3263/$ – see front matter © 2007 Elsevier Inc. All rights reserved.
doi:10.1016/j.jmgm.2007.06.001

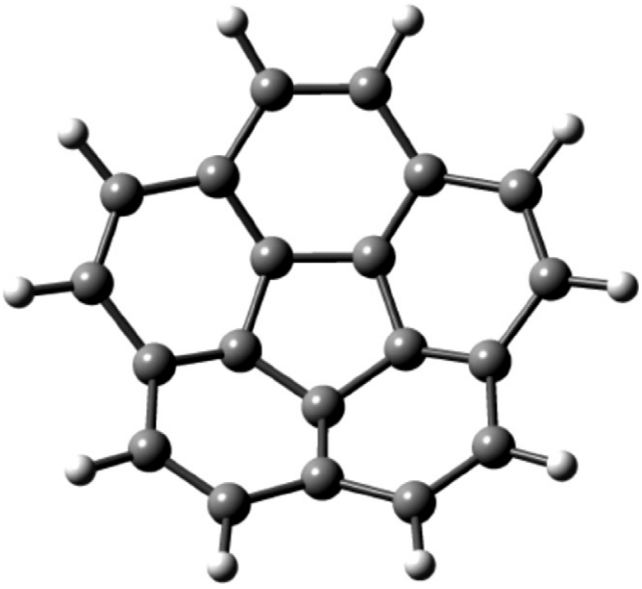

Fig. 1. The structure of corannulene $C_{20}H_{10}$.

isomer 1 and isomer 2 converge at D_{3h} and D_{3d} group points, respectively. On the basis of the optimized geometry, vibrational frequencies and the magnetic shielding tensors of the two isomers of the molecule $C_{40}O_{10}$ were computed at the B3LYP/6-31G* level of theory, too. Vibrational frequencies were determined firstly to verify the nature of stationary points, second to use the sum of electronic and thermal enthalpy that includes electronic energy and translational, rotational, and thermal vibrational corrections for calculating the heat of formation of the molecule, and third to predict vibrational frequencies of the unknown stable species for the sake of their future experimental identification by infrared (IR) spectroscopy and the assignment of the observed frequencies. For future experimental identification of the two isomers by NMR, their magnetic shielding tensors were calculated by using the gauge-including-atomic-orbital (GIAO) method and the continuous-set-of gauge-transformation (CSGT) procedure [5]. In order to understand the electronic and reactive properties, the net charges with natural bond orbital method and the probability density surfaces corresponding to the HOMO and the LUMO molecular orbitals have been studied, too.

Table 1
Optimized equilibrium geometries of the two isomers of $C_{40}O_{10}$ at the B3LYP/6-31G* level of theory

Isomer	Bond lengths (Å)	Bond angles (°)
1	C_1–C_2: 1.443 C_1–C_9: 1.418 C_6–C_7: 1.438 C_7–C_8: 1.380 C_7–O_{22}: 1.403	$\angle C_1C_2C_3$: 108.0; $\angle C_1C_5C_6$: 121.2 $\angle C_5C_6C_7$: 116.5; $\angle C_6C_7C_8$: 122.1 $\angle C_6C_7O_{22}$: 119.0; $\angle C_7C_6C_{20}$: 120.2 $\angle C_7C_8O_{23}$: 112.0; $\angle C_7O_{22}C_{34}$: 104.1
2	C_1–C_2: 1.441 C_1–C_9: 1.412 C_6–C_7: 1.443 C_7–C_8: 1.380 C_7–O_{22}: 1.401	$\angle C_1C_2C_3$: 108.0; $\angle C_1C_5C_6$: 121.3 $\angle C_5C_6C_7$ 116.5; $\angle C_6C_7C_8$: 122.0 $\angle C_6C_7O_{22}$: 119.4; $\angle C_7C_6C_{20}$: 119.9 $\angle C_7C_8O_{23}$: 113.0; $\angle C_7O_{22}C_{34}$: 103.5

3. Bonding and net charge

We began our study by structural optimization of pure C_{60} at the B3LYP/6-31G* level of theory. The calculated bond lengths for 6–6 bonds (hexagon–hexagon) and 5–6 bonds (pentagon–hexagon) are 1.395 and 1.453 Å, respectively, which are in reasonable agreement with the experimental values reported in Ref. [6]. This shows that the DFT method at the B3LYP/6-31G* level of theory is suitable for studying the cage-like molecule.

We use two-dimensional schematic views (Fig. 3.) to show how polygons can be distributed in the two isomers of $C_{40}O_{10}$. The optimized bond lengths and bond angles are given in Table 1 with the numbering system of carbon and oxygen atoms in Fig. 3. We find that the two isomers all have only one unique C–O bond lengths about 1.40 Å and four unique C–C bond lengths in the range of 1.380–1.443 Å. The longest C–C bonds are all C–C bonds forming pentagons, which lengths are about 1.44 Å; the shortest C–C bonds are C–C (7–8, 10–11, 13–14, 16–17, 19–20, 31–45, 33–34, 36–37, 39–40, 42–43) bonds, which lengths are about 1.38 Å.

The distances (or radii) R_i from the ith atom to the density center of the molecule $C_{40}O_{10}$ are listed in Table 2. We find that $C_{40}O_{10}$ is an oblate sphere with four unique radii, and the longest radius is radius of each oxygen atom with about 4.0 Å, and the shortest radius is radius of each carbon atom formed the pentagons with about 2.6 Å.

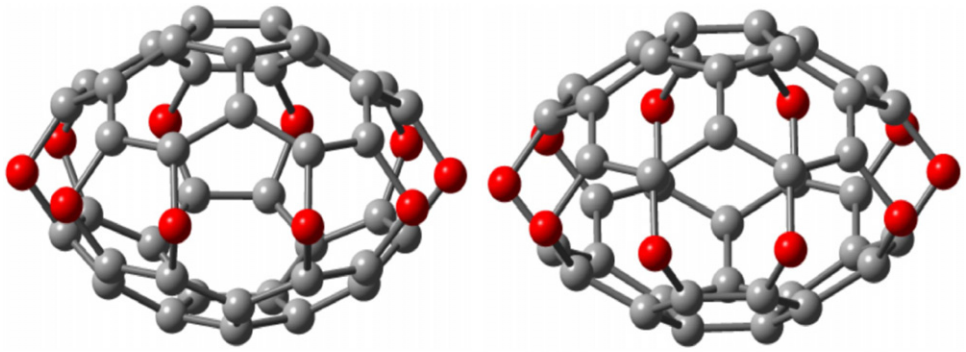

Fig. 2. The structures of two isomers of $C_{40}O_{10}$.

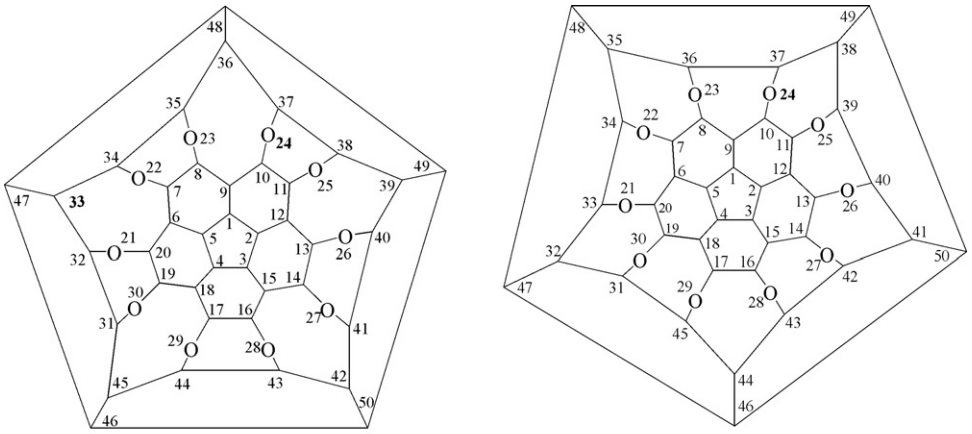

Fig. 3. Numbering system of atoms in the two isomers of $C_{40}O_{10}$.

Table 2
B3LYP/6-31G* calculations of radius (R_i, in Å) and net charge (Q_i, in e, where 1e = 1.6×10^{-16} C) for the two isomers of $C_{40}O_{10}$

Species	Site number $\{n_i\}$	Atom	R_i	Q_i
Isomer 1	{1, 2, 3, 4, 5, 46, 47, 48, 49, 50}	C	2.663	−0.009
	{6, 9, 12, 15, 18, 33, 36, 39, 42, 45}	C	2.998	−0.085
	{7, 8, 10, 11, 13, 14, 16, 17, 19, 20, 31, 32, 34, 35, 37, 38, 40, 41, 43, 44}	C	3.336	0.301
	{21, 22, 23, 24, 25, 26, 27, 28, 29, 30}	O	3.947	−0.506
Isomer 2	{1, 2, 3, 4, 5, 46, 47, 48, 49, 50}	C	2.614	−0.003
	{6, 9, 12, 15, 18, 32, 35, 38, 41, 44}	C	2.975	−0.095
	{7, 8, 10, 11, 13, 14, 16, 17, 19, 20, 31, 33, 34, 36, 37, 39, 40, 42, 43, 45}	C	3.325	0.305
	{21, 22, 23, 24, 25, 26, 27, 28, 29, 30}	O	4.004	−0.512

Since the hybrids of all carbon are sp^2 and all oxygen atoms are sp^3, apart from the ∠CCC angles of pentagons at the two ends of each isomer's cage (the value of ∠CCC is 108°), other bond angles ∠CCC of them obtained at the B3LYP/6-31G* level of theory are close to 120° and all bond angles ∠COC are close to ∠HOH of H_2O (the value is 104.5°). Thus, most of the strain energies of the two isomers are from the pentagons at the two ends of each isomer's cage, and the strain energies of other polygons are very small.

Unfortunately, there is no single way in which to derive accurate electron populations at atoms, different methods lead to different populations. Here we use the Weinhold's natural population analysis (NPA) [7], which is based on the NBO procedure, to gain the net atomic charges Q_i in the two isomers. Symmetry requires that all oxygen atoms have the same charge density, but the carbon atoms have three unique atomic net charges. Table 2 lists the NPA charges Q_i for unique atoms of the two isomers. According to the results in Table 2, all oxygen atoms have very large negative net charges (about −0.5e), and the carbon atoms linked to oxygen atoms directly have large positive net charges (about 0.3e), other carbon atoms have very small positive charges.

Fig. 4 presents the HOMO and LUMO molecular orbitals of the two isomers. For isomer 1, the HOMO orbital has E_1'' symmetry and its energy is −6.81 eV, the LUMO orbital has E_1' symmetry and its energy is −3.46 eV. For isomer 2, the HOMO orbital has E_{2g} symmetry and its energy is −6.79 eV, the LUMO orbital has E_{1g} symmetry and its energy is −3.64 eV. We find that frontier orbitals (HOMO and LUMO) of the two isomers have less contribution from the oxygen atoms, thus all oxygen atoms are not active site to act as electron-acceptor partners or act as electron-donor partners.

4. Vibrational frequency

To verify whether the two isomers of $C_{40}O_{10}$ are real minima on the potential energy hypersurface, vibrational frequencies have been calculated at the B3LYP/6-31G* level of theory. The predicted, unscaled vibrational frequencies are listed in Table 3. The absences of imaginary vibrational frequencies confirm that the two isomers of $C_{40}O_{10}$ correspond to true minima on the potential energy hypersurface.

Symmetries (D_{5h} and D_{5d}) of the two isomers are helpful in making the assignments of their vibrational frequencies. The reducible representation of vibrational motions of isomer 1 is therefore reduced to

$$\Gamma_{\text{vib}} = 9A_1'(\text{R}) + 6A_2' + 15E_1'(\text{IR}) + 16E_2'(R) + 6A_1'' + 7A_2''(\text{IR}) + 13E_1''(\text{R}) + 14E_2''$$

of which the E_1'' and A_2'' are infrared active, and the other normal modes are all infrared forbidden by symmetry and their infrared

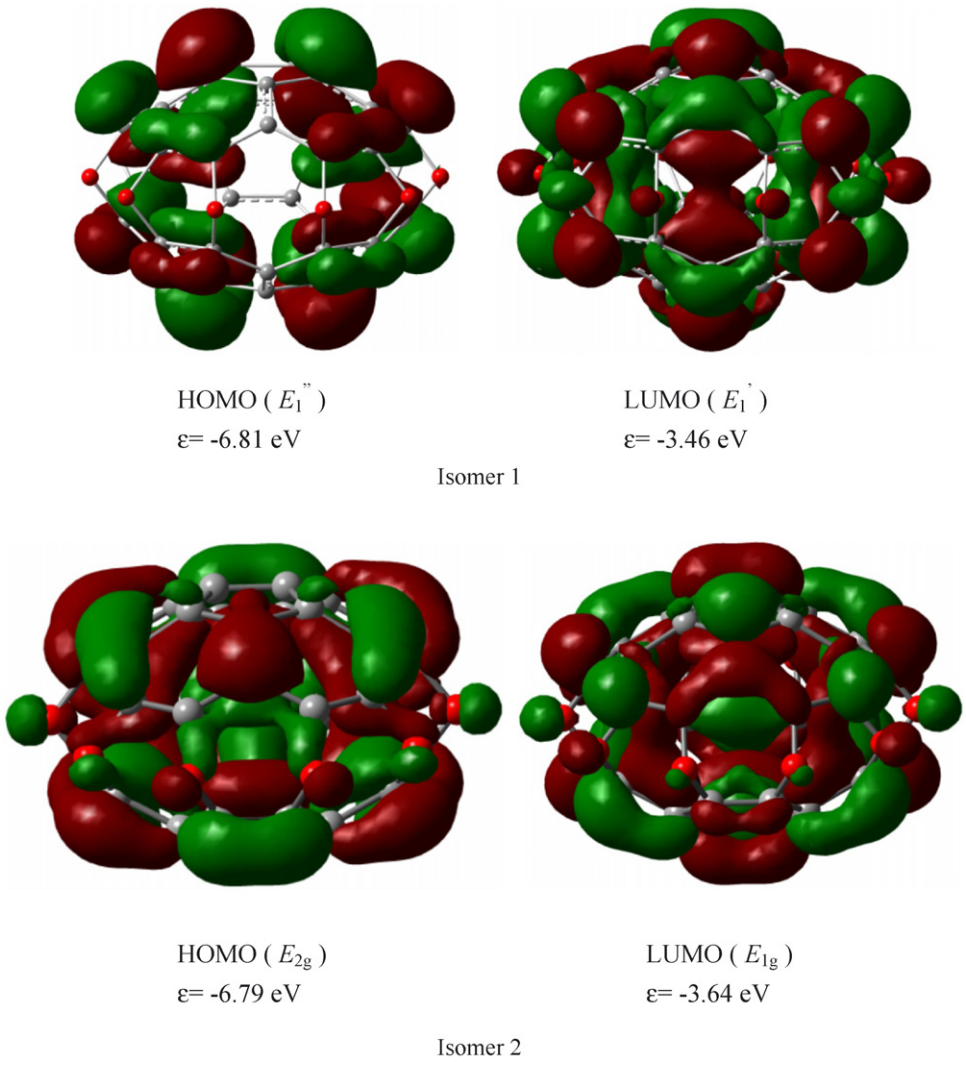

Fig. 4. The HOMO and LUMO molecular orbitals of $C_{40}O_{10}$.

Table 3
Vibrational frequencies[a] and the active infrared (IR) intensities of the two isomers of $C_{40}O_{10}$ calculated at the B3LYP/6-31G* level of theory

Isomer 1	
A_1'	216.5, 486.7, 550.3, 619.1, 775.0, 931.5, 1264.8, 1416.9, 1609.1
A_2'	406.1, 595.8, 745.1, 867.3, 1156.1, 1466.7
E_1'	310.6 (2.1)[b], 398.2 (2.7), 441.0 (1.5), 568.7 (36.7), 589.5 (1.0), 611.2 (5.8), 702.1 (26.6), 774.8 (17.7), 857.4 (3.8), 1069.3 (15.0), 1115.4 (106.8), 1349.1 (89.5), 1375.9 (2.8), (0.0), 1436.5 (7.7), 1609.8 (13.3)
E_2'	309.9, 387.0, 403.9, 514.2, 566.8, 731.6, 782.5, 792.2, 904.2, 1042.5, 1201.0, 1302.9, 1357.5, 1427.3, 1462.6, 1568.5
A_2''	349.9, 564.3, 670.9, 808.2, 1071.3, 1459.8
A_2''	358.8 (8.9), 533.8 (2.5), 687.5 (3.6), 984.8 (153.3), 1240.4 (416.1), 1407.1 (85.7), 1579.4 (97.9)
E_1''	233.2, 425.8, 512.4, 607.1, 648.4, 718.9, 748.7, 1028.2, 1098.7, 1285.3, 1365.2, 1408.7, 1586.8
E_2''	266.4, 379.3, 446.0, 490.4, 648.4, 688.9, 722.4, 790.7, 898.9, 995.9, 1158.7, 1267.3, 1310.2, 1548.2
Isomer 2	
A_{1g}	210.8, 429.5, 548.7, 767.9, 947.3, 1248.6, 1422.8, 1611.2
A_{2g}	494.9, 603.3, 666.9, 816.4, 1079.7, 1440.7
E_{1g}	241.2, 445.3, 530.3, 639.1, 729.8, 748.0, 806.0, 862.9, 1082.7, 1187.3, 1265.8, 1427.9, 1579.2, 1598.7
E_{2g}	308.5, 381.0, 456.5, 476.4, 479.7, 566.6, 692.3, 757.8, 816.4, 1024.9, 1122.1, 1331.5, 1364.8, 1370.8, 1434.9
A_{1u}	397.6, 524.2, 756.0, 832.2, 1170.8, 1451.6
A_{2u}	361.8 (7.9), 510.7 (3.3), 585.5 (0.1), 699.1 (0.9), 986.4 (113.0), 1278.1 (413.7), 1416.4 (69.0), 1604.0 (109.3)
E_{1u}	307.5 (0.0), 390.9 (4.1), 463.0 (3.2), 581.9 (8.5), 612.6 (1.2), 644.2 (27.9), 750.9 (70.3), 787.2 (4.1), 1045.7 (28.4), 1110.1 (93.2), 1313.7 (98.3), 1361.6 (1.3), 1427.8 (42.8), 1609.4 (29.8)
E_{2u}	286.0, 386.6, 410.8, 479.1, 602.2, 735.5, 767.7, 806.6, 909.9, 1016.5, 1184.6, 1303.4, 1336.9, 1458.1, 1563.7

[a] The unit of vibrational frequencies is cm^{-1}.
[b] The unit of IR intensity of active mode is km mol^{-1}, and given in the parentheses. The IR intensities of all inactive modes are all zero, and not given in this table.

intensities are all zero. Here we discuss several vibrational bands in the IR intensity of isomer 1 to be compared with future experimental identification: (i) the strongest IR spectroscopic signal with IR intensity of 416.1 km mol^{-1} is determined at the frequency 1240.4 cm^{-1}; (ii) three strong modes are observed are frequencies 984.8, 1115.4, and 1349.1 cm^{-1} with IR intensities of 153.3, 213.6, and 179.1 km mol^{-1}, respectively; (iii) five intermediate modes appear at frequencies 568.7, 702.1, 774.8, 1407.1, and 1579.4 with IR intensities of 73.8, 53.1, 35.4, 85.7, and 97.9 km mol^{-1}, respectively.

The A'_1, E'_2 and E''_1 vibrational modes of isomer 1 are Raman active.

The reducible representation of vibrational motions of isomer 2 is therefore reduced to

$$\Gamma_{\text{vib}} = 8A_{1g}(\text{R}) + 6A_{2g} + 14E_{1g}(\text{R}) + 15E_{2g}(\text{R}) + 6A_{1u} + 8A_{2u}(\text{IR}) + 14E_{1u}(\text{IR}) + 15E_{2u}$$

of which the A_{2u} and E_{1u} are infrared active, and the other normal modes are all infrared forbidden by symmetry and their infrared intensities are all zero. Here we discuss several vibrational bands in the IR intensity of isomer 2 to be compared with future experimental identification: (i) the strongest IR spectroscopic signal with IR intensity of 413.7 km mol^{-1} is determined at the frequency 1278.1 cm^{-1}; (ii) five strong modes are observed are frequencies 750.9, 986.4, 1110.1, 1313.7, and 1604.0 cm^{-1} with IR intensities of 140.6, 113.0, 186.4, 196.6, and 109.3 km mol^{-1}, respectively; (iii) four intermediate modes appear at frequencies 644.2, 1045.7, 1416.4, and 1427.8 with IR intensities of 55.8, 56.8, 69.1, and 85.6 km mol^{-1}, respectively.

The A_{1g}, E_{1g}, and E_{2g} vibrational modes of isomer 2 are Raman active.

We used frequencies and IR intensities in Table 3 to simulate IR spectra of isomers 1 and 2, see Fig. 5. The simulated IR spectra could be used as evidence to identify the two isomers of $C_{40}O_{10}$.

5. Magnetic shielding tensors

For future experimental identification of the two isomers by NMR, their magnetic shielding tensors σ were calculated by using the gauge-including-atomic-orbital (GIAO) method and the continuous-set-of gauge-transformation (CSGT) procedure [5], which is implemented in GAUSSIAN 98 program [4]. In high-resolution NMR, the isotropic part σ_{iso} of σ is measured by taking the average of σ with respect to the orientation to the magnetic field, i.e., $\sigma_{\text{iso}} = (\sigma_{xx} + \sigma_{yy} + \sigma_{zz})/3$, where σ_{xx}, σ_{yy}, and σ_{zz} are the principal axis values of σ. The results calculated by using B3LYP hybrid DFT and restricted Hartree–Fock (RHF) theory are summarized in Table 4. As for comparison, the isotropic part σ_{iso} of ^{13}C in the reference tetramethylsilane (TMS) also listed in Table 4.

We find that the each isomer of $C_{40}O_{10}$ has three ^{13}C and one ^{17}O NMR spectral signals, indicative of the four unique sites in each isomer of $C_{40}O_{10}$ structure. In isomer 1, the NMR spectral signal of ^{13}C {1, 2, 3, 4, 5, 46, 47, 48, 49, 50} is very close to that of ^{13}C {6, 9, 12, 15, 18, 33, 36, 39, 42, 45}, but in isomer 2, the two NMR spectral signals is not close each other. This can be used to distinguish the isomers 1 and 2.

The Ref. [8] pointed out the DFT method does not provide systematically better NMR results than RHF and the CSGT procedure provides better NMR results than GIAO procedure. So we calculated the ^{13}C NMR chemical shift $\delta = \sigma_{\text{iso}}^{\text{TMS}} - \sigma_{\text{iso}}^{\text{sample}}$ with respect to the reference tetramethysilane (TMS) for the two isomers of $C_{40}O_{10}$ at the RHF/6-31G* level of theory by using the CSGT method, also listed in Table 4.

6. The estimation of heat of formation

What is the stability of the two isomers of $C_{40}O_{10}$. To answer this, the approach calculates the energy change of the homodesmic reaction (1) in ΔH_{r} from the sum of electronic and thermal enthalpies at 298 K computed at the B3LYP/6-31G* level of theory:

$$2C_{60} + 60CH_3OH = 3C_{40}O_{10} + 30CH_3{-}CH_3 + 30H_2O \quad (1)$$

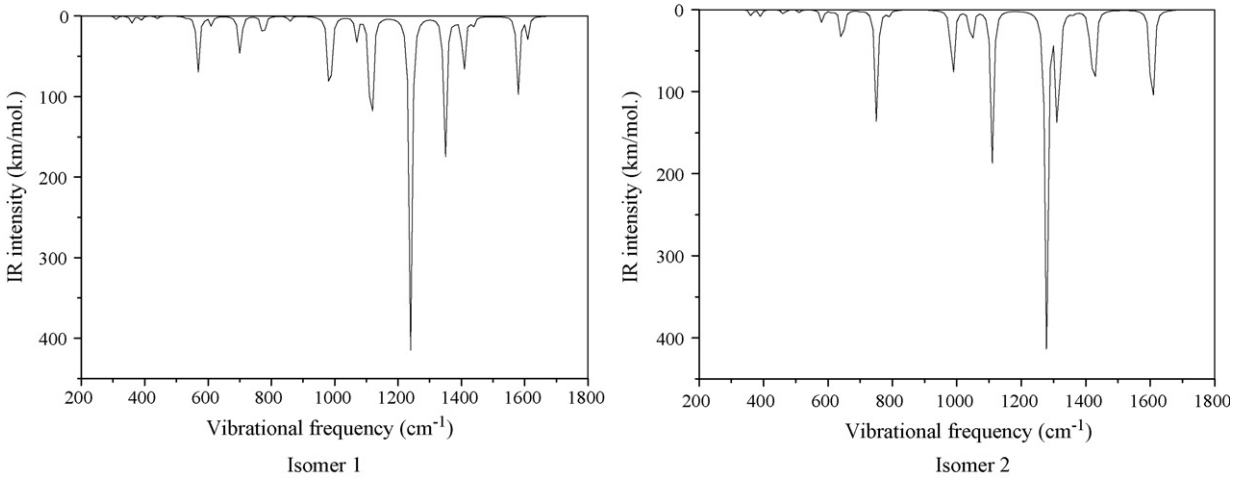

Fig. 5. Simulated IR spectra of the two isomers of $C_{40}O_{10}$.

Table 4
B3LYP/6-31G* and RHF/6-31G* calculations of the absolute isotropy, σ_{iso} in ppm (parts per million), of the nuclear magnetic shielding tensor σ for atoms in the two isomers of $C_{40}O_{10}$ and tetramethysilane (TMS) found by using both GIAO and CSGT methods

Species	Site number $\{n_i\}$	σ_{iso}				
		σ_{iso}[a]	σ_{iso}[b]	σ_{iso}[c]	σ_{iso}[d]	δ (ppm)[e]
Isomer 1	^{13}C {1, 2, 3, 4, 5, 46, 47, 48, 49, 50}	54.2	49.2	58.0	51.8	145.1
	^{13}C {6, 9, 12, 15, 18, 33, 36, 39, 42, 45}	55.6	49.8	56.6	50.1	146.8
	^{13}C {7, 8, 10, 11, 13, 14, 16, 17, 19, 20, 31, 32, 34, 35, 37, 38, 40, 41, 43, 44}	17.3	10.3	25.1	17.0	179.9
	^{17}O {21, 22, 23, 24, 25, 26, 27, 28, 29, 30}	162.5	154.0	216.9	206.4	
Isomer 2	^{13}C {1, 2, 3, 4, 5, 46, 47, 48, 49, 50}	53.3	48.5	55.9	50.1	146.8
	^{13}C {6, 9, 12, 15, 18, 32, 35, 38, 41, 44}	66.5	60.8	65.8	59.4	137.5
	^{13}C {7, 8, 10, 11, 13, 14, 16, 17, 19, 20, 31, 33, 34, 36, 37, 39, 40, 42, 43, 45}	21.3	14.8	33.6	25.8	171.1
	^{17}O {21, 22, 23, 24, 25, 26, 27, 28, 29, 30}	192.2	181.7	243.8	231.6	
TMS	^{13}C	189.8	188.6	200.0	196.9	

[a] The σ_{iso} obtained at the B3LYP/6-31G* level of theory by using the GIAO method.
[b] The σ_{iso} obtained at the B3LYP/6-31G* level of theory by using the CSGT method.
[c] The σ_{iso} obtained at the RHF/6-31G* level of theory by using the GIAO method.
[d] The σ_{iso} obtained at the RHF/6-31G* level of theory by using the CSGT method.
[e] $\delta = \delta_{iso}^{TMS} - \delta_{iso}^{sample}$ is at the RHF/6-31G* level of theory by using the CSGT method and its unit is parts per million (ppm).

where the sum of electronic and thermal enthalpies of each molecule includes electronic energy and translational, rotational, and thermal vibrational corrections. The energy change ΔH_r of the homodesmic reaction (1) and the gaseous heats of formation ΔH_f° of methanol, ethane, and water lead to ΔH_f° of the two isomers of $C_{40}O_{10}$. The data used to calculate ΔH_f° of the two isomers are listed in Table 5.

The energy changes ΔH_r of the homodesmic reaction (1) for isomers 1 and 2 are −57.4 and −85.4 kcal/mol, respectively.

Using the ΔH_r of the homodesmic reaction (1) and gaseous heats of formation of methanol, ethane, water and C_{60} in Table 5, the ΔH_f° of isomers 1 and 2 can be estimated by

$$\Delta H_{f,C_{40}O_{10}} = \frac{2\Delta H_{f,C_{60}}^\circ + 60\Delta H_{f,methanol}^\circ - 30\Delta H_{f,ethane}^\circ - 30\Delta H_{f,water}^\circ + \Delta H_r}{3} \quad (2)$$

The ΔH_f° of isomers 1 and 2 at 298 K are 205.3 and 195.9 kcal/mol, respectively.

We also used the following reaction (3) to estimate ΔH_f° of the two isomers of $C_{40}O_{10}$:

$$2C_{60} + 15O_2 = 3C_{40}O_{10} \quad (3)$$

Table 5
The electronic and thermal enthalpies (SETE) and the gaseous experimental ΔH_f° of methanol, ethane, water, C_{60}[a] and the SETE of the two isomers of $C_{40}O_{10}$ at 298 K

Molecule	SETE (a.u.)	ΔH_f° (kcal mol^{-1})
Methanol	−115.65870	−48.1
Ethane	−79.75076	−20.2
Water	−76.38401	−57.8
C_{60}	−2285.77368	609.6
Isomer 1	−2275.70589	
Isomer 2	−2275.72077	

[a] The experimental ΔH_f° of methanol, ethane, water were taken from Ref. [9], and the experimental ΔH_f° of C_{60} was taken from Ref. [10].

The values for isomers 1 and 2 are 223.2 and 213.8 kcal/mol, respectively, which coincide with the results of the homodesmic reaction (1).

Since the estimated ΔH_f° of the two isomers of $C_{40}O_{10}$ at 298 K are very lower than that of C_{60} and C_{60} is a stable molecule, they are all stable molecules only from the thermodynamic points of view. Thus, we believe that the two isomers of $C_{40}O_{10}$ have sufficient stability to allow their experimental preparation.

7. Summary

In summary, we have performed DFT calculations of bonding, natural population analysis, vibrational frequencies, IR intensities, magnetic shielding tensors, and heats of formation of the two isomers of $C_{40}O_{10}$. Each isomer has 22 IR-active independent vibrational modes. Isomer 1 has 38 and isomer 2 has 37 Raman-active independent vibrational modes, respectively. All IR- and Raman-active vibrational frequencies are assigned. Three ^{13}C and one ^{17}O NMR spectral lines for each isomer are characterized. Heat of formation of each isomer is estimated. Compared the stability of the two isomers of $C_{40}O_{10}$ with that of C_{60}, only from the thermodynamic points of view, they are more stable than C_{60}. Thus, we believe that they have sufficient stability to allow their experimental preparation.

Acknowledgement

We appreciate the financial support of this work that was provided by Natural Science Foundation Committee of China (No. 60671010).

References

[1] W.E. Barth, R.G. Lawton, J. Am. Chem. Soc. 93 (1973) 370.
[2] A.D. Becke, J. Chem. Phys. 98 (1993) 5648.

[3] (a) G. Trinquier, J.P. Malrieu, J.P. Daudey, Chem. Phys. Lett. 80 (1981) 552;
(b) G. Trinquier, J.P. Daudey, N. Komiha, J. Am. Chem. Soc. 107 (1985) 7210;
(c) R. Ahlrichs, S. Brode, C. Ehrhardt, J. Am. Chem. Soc. 107 (1985) 7260.

[4] M.J. Frisch, G.W. Trucks, H.B. Schlegel, G.E. Scuseria, M.A. Robb, J.R. Cheeseman, V.G. Zakrzewski, J.A. Montgomery Jr., R.E. Stratmann, J.C. Burant, S. Dapprich, J.M. Millam, A.D. Daniels, K.N. Kudin, M.C. Strain, O. Farkas, J. Tomasi, V. Barone, M. Cossi, R. Cammi, B. Mennucci, C. Pomelli, C. Adamo, S. Clifford, J. Ochterski, G.A. Petersson, P.Y. Ayala, Q. Cui, K. Morokuma, D.K. Malick, A.D. Rabuck, K. Raghavachari, J.B. Foresman, J. Cioslowski, J.V. Ortiz, B.B. Stefanov, G. Liu, A. Liashenko, P. Piskorz, I. Komaromi, R. Gomperts, R.L. Martin, D.J. Fox, T. Keith, M.A. Al-Laham, C.Y. Peng, A. Nanayakkara, C. Gonzalez, M. Challacombe, P.M.W. Gill, B. Johnson, W. Chen, M.W. Wong, J.L. Andres, C. Gonzalez, M. Head-Gordon, E.S. Replogle, J.A. Pople, Gaussian 98, Revision A.3, Gaussian, Inc., Pittsburgh, PA, 1998.

[5] J.R. Cheeseman, M.J. Frisch, G.W. Trucks, T.A. Keith, J. Chem. Phys. 104 (1996) 5497.

[6] W.I.F. David, R.M. Ibberson, J.C. Matthew, K. Pressides, T.J. Dannis, J.P. Hare, H.W. Kroto, R. Taylor, D.C.M. Walton, Nature 353 (1991) 147.

[7] (a) D.W. Schwenke, D.G. Truhlar, J. Chem. Phys. 82 (1985) 2418;
(b) M.J. Frisch, J.E. DelBene, J.S. Binkley, H.F. Schaefer III, J. Chem. Phys. 84 (1986) 2279;
(c) M. Gutowski, J.G.C.M. van Duijneveldt-van de Rijdt, J.H. van Lenthe, F.B. van Duijneveldt, J. Chem. Phys. 98 (1993) 4728;
(d) M. Gutowski, G.J. Chalasinski, J. Chem. Phys. 98 (1993) 5540;
(e) J.H. van Lenthe, J.G.C.M. van Duijneveldt-van de Rijdt, F.B. van Duijneveldt, in: K.P. Lawley (Ed.), Ab Initio Methods in Quantum Chemistry II, Wiley & Sons Ltd., London, 1987, p. 521;
(f) A.E. Reed, L.A. Curtiss, F. Weinhold, Chem. Rev. 88 (1988) 899;
(g) J.E. Carpenter, F. Weinhold, J. Mol. Struct. (Theochem.) 169 (1988) 41.

[8] R.-H. Xie, L. Jensen, G.W. Bryant, J. Zhao, V.H. Smith Jr., Chem. Phys. Lett. 375 (2003) 445.

[9] R.C. Weast, CRC Handbook of Chemistry and Physics, 60th ed., CRC Press, Boca Raton, FL, 1980.

[10] H.-D. Beckhaus, S. Verevkin, C. Rüchardt, F. Diederich, C. Thilgen, H.-U. ter Meer, H. Mohn, W. Müller, Angew. Chem. Int. Ed. Engl. 33 (1994) 996.